Lawrence Berkeley Laboratory
UNIVERSITY OF CALIFORNIA

Invited paper presented at the Workshop on Quark Matter Formation and Heavy Ion Collisions, Bielefeld, West Germany, May 10-14, 1982

RECENT RESULTS FROM THE BEVALAC

Howel G. Pugh

June 1982

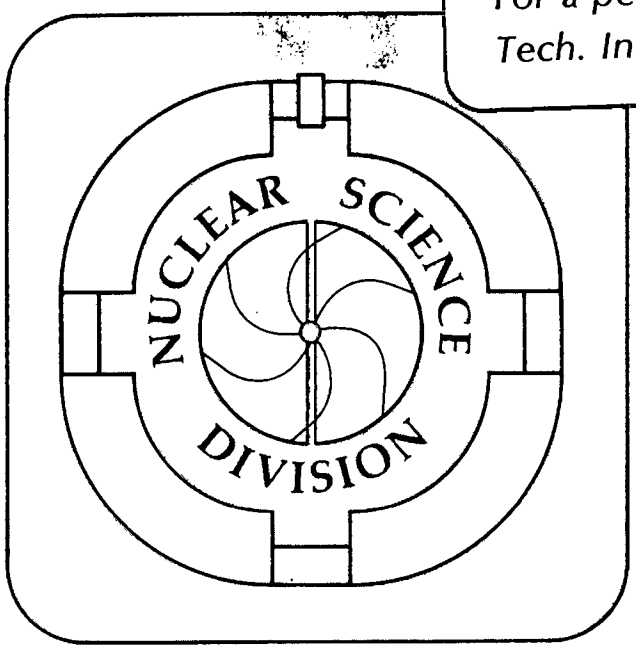

Prepared for the U.S. Department of Energy under Contract DE-AC03-76SF00098

DISCLAIMER

LBL-14513

RECENT RESULTS FROM THE BEVALAC

Invited paper presented at the Workshop
on Quark Matter Formation and Heavy Ion Collisions

Bielefeld, May 10-14, 1982

Howel G. Pugh

Nuclear Science Division
Lawrence Berkeley Laboratory
University of California
Berkeley, CA 94720

This work was supported by the Director, Office of Energy Research, Office of Nuclear Physics of the Office of High Energy and Nuclear Physics of the U.S. Department of Energy under Contract DE-AC03-76SF00098.
This manuscript was printed from originals provided by the author.

LBL-14513

RECENT RESULTS FROM THE BEVALAC

Howel G. Pugh
Nuclear Science Division, Lawrence Berkeley Laboratory
University of California, Berkeley, CA 94720

"We shall not cease from exploration
And the end of all our exploring
Will be to arrive where we started
And know the place for the first time."

T.S. Eliot: Four Quartets

1. Introduction

The Bevalac provides beams of nuclei up to kinetic energies of 2.1 GeV/amu. Research using these beams concerns the properties of nuclei, the properties of nuclear matter, and the properties of nuclei under extreme conditions of density and temperature. The new questions that arise in this regime are of considerable interest: Can a pion condensation occur? Can density isomers be produced? Can one produce transitions to new phases of nuclear matter involving hadronic or quark-gluon degrees of freedom? Experimental and theoretical studies in these directions widen our horizons, clarify our understanding, and may indeed lead to our knowing the nucleus for the first time.

In this talk I will not attempt to discuss the majority of data from the Bevalac. I restrict myself to the past year, to a few topics of special relevance to the subject of this Workshop, and to an indication of the prospects for progress in the next few years. Because of its special potential importance, I will give an assessment of the current state of knowledge concerning anomalous projectile fragments (anomalons).

2. Selected Experimental Topics

Figure 1 shows a streamer chamber photograph of a collision between a 1.8 GeV/amu argon ion and a lead target. How can we hope to learn anything at all by studying such collisions?

Fortunately, we have learned that great simplicities exist. The most useful one is the approximate separation of participant and spectator regions of the interacting nuclei. Figure 2 shows schematically how this occurs. The overlapping regions of projectile and target undergo violent interaction while the non-overlapping regions either continue with beam velocity and break up into "projectile fragments" or remain at rest and break into "target fragments". Projectile fragments are the easiest to study; the participants, in the mid-rapidity region, are the next easiest, while the target fragments have not been extensively studied, except by radiochemistry techniques.

In this talk I will concentrate (with the exception of a discussion of anomalous projectile fragments) on the participant region, where we would expect to find high densities and temperatures and where we will have to look to find evidence of any phase transition. I will have to omit the extensive evidence for a high degree of equilibration at Bevalac energies, even though the stopping power of nuclei is crucial for possible studies at higher energies. Results are accumulating sufficiently rapidly that this might be the primary topic for discussion at the next Workshop.

2a. Inclusive Spectra

In the past year a major paper has been published by Nagamiya et al.[1] on the large angle inclusive spectra of p, d, t, ^{3}He, π, and K^+. I have selected some data at $\theta_{cm} = 90°$ to reflect the participant region.

Figure 3 shows proton spectra. The curve given for single nucleon-nucleon scattering with Fermi distributions folded in does not suffice to describe the data. In order to fit the exponential tails of the spectra, it is necessary to include up to 4-5 multiple scatterings at 0.8 GeV/A. In the limit such scatterings might converge to an equilibrium situation represented by a temperature. Figure 4 shows pion spectra at a number of beam energies. In every

case the spectrum has an exponential form. Figure 5 shows the K^+ inclusive cross section[2]. Here the angular distribution is almost isotropic in the cm frame and the spectra at all angles fall on a single exponential, which is not the case for pions and protons.

Nagamiya et al. used the inverse of the exponential slope to systematize the data, as shown in Figure 6. These slopes have a general relationship to the temperature reached in the collision, as has been discussed by Stocker, Ogloblin and Greiner[3]. Nagamiya and Gyulassy[4] have pointed out that the inverse slope E_o increases as we go from π to p to K, which is in the sequence neither of the masses nor of the amount of available phase space. They suggest that the explanation is to be found in the interaction mean free paths for the secondary particles, which at these energies increase in the sequence π:p:K. The kaons therefore may reflect most closely some primordial temperature while the pions reflect the final expansion phase of the collision. Similar ideas were presented in reference 5 where Λ production in central collisions was found to result in very large longitudinal and transverse momenta. The mean free path for Λs is also very long at Bevalac energies.

Nagamiya has proposed the conceptual hybrid scheme shown in Figure 7. According to this some high density state is formed in the collision, which is probed most accurately by long mean free path particles. Rafelski[6] has recently analyzed the K^+, Λ, and recent K^- data[7] in terms of average transverse momenta to extract temperatures in the region of 120 MeV.

2b. Two Pion Intensity Interferometry

This technique for heavy ion collisions was introduced by Fung et al.[8] using a streamer chamber. Recently data with higher statistical accuracy have been obtained electronically by Zajc et al.[9] for Ar + KCl collisions at 1.8 GeV/amu.

Zajc et al. measure the correlation function

$$C_2(\vec{p}_1,\vec{p}_2) = \frac{N(\vec{p}_1,\vec{p}_2)}{N(\vec{p}_1)\,N(\vec{p}_2)} \quad .$$

$$C_2(\vec{p}_1,\vec{p}_2) = 1 + \lambda \exp\left[-\frac{1}{2}(\vec{p}_1 - \vec{p}_2)^2R^2 - \frac{1}{2}(E_1 - E_2)^2T^2\right]$$

The quantity R represents a radius parameter for the source, T a time parameter (not found to be important in fitting the data), and λ the degree of incoherence (λ = 1 representing a fully incoherent source).

Figure 8 and Table I show fits to the $2\pi^-$ and $2\pi^+$ data at 90° cm. The comparison between Figs. 8a,8b shows the effect of final state Coulomb interactions between the pions, which must be allowed for. Figures 8c and 8d show fits with the coherence parameter λ and the radius parameter R as free parameters. There is some evidence for a deviation from complete incoherence. For a recent discussion of the possible origins of such deviations see Gyulassy[10]. Results on central ^{40}Ar + KCl collisions will soon be available from the streamer chamber.

Lu et al.[11] have recently published new data on ^{40}Ar + Pb at 1.8 GeV/amu. They explore the dependence of R on the pion multiplicity as shown in Figure 9. The increase with n_π is consistent with the known relationship between n_π and the participant number. Large participant numbers correspond to small impact parameters and large source sizes.

2c. Exclusive Charged Particle Measurements: Plastic Ball

The simplified picture of a heavy ion collision that was discussed in the beginning of this section does not allow for collective effects. Figure 10 shows the results of a hydrodynamical calculation[12] in which the projectile and target fragments receive sideways kicks while the participants also have a distinctive velocity distribution. Testing such mechanisms requires multiparticle correlation measurements. To perform such measurements a GSI-LBL collaboration built the Plastic Ball-Wall array shown in Figure 11.

The main part of the Ball has the same geometric configuration as the Crystal Ball at SLAC. The forward part is, however, more finely segmented and the Plastic Wall, 6 m downstream from the target, provides excellent angular resolution in the projectile fragmentation region. Figure 12 shows one element of the Plastic Ball. The ΔE and E signals are measured with the same phototube and resolved by pulse shape analysis. A delayed signal also identifies

stopping π^+. Figure 13 shows the discrimination obtained between particles.

There has been one data run with the Plastic Ball-Wall, and data are just beginning to emerge. Figure 14 shows the deuteron-proton ratio as a function of the total charged multiplicity. It is useful to think of this in terms of a coalescence model. Under certain assumptions the chance of coalescence of a neutron and a proton to form a deuteron would be proportional to the square of the multiplicity and the d-p ratio would depend linearly on the multiplicity as observed. This is consistent with a result obtained by Nagamiya et al.[1] who found, as shown in Figure 15, that the deuteron inclusive spectra can be fitted exactly by the square of the proton spectra with a single adjusted normalization factor, which is the same at all angles. The Plastic Ball-Wall will obviously provide comprehensive information on this as well as many other phenomena.

It should be noted that, according to this simplest model of coalescence, the probability of forming a nucleus of mass A is proportional to the nucleon multiplicity to the Ath power. By analogy, production of composite multiquark objects at very high energies may depend on multiplicity in a corresponding way. Since the multiplicities may be of the order of several thousand we may see a large enhancement of composite particle production at nucleus-nucleus colliding beam facilities.

2d. Exclusive Charged Particle Measurements: Streamer Chamber

Though the Plastic Ball will eventually give 4π data with excellent statistics, it is to the streamer chamber that we owe the first glance at this kind of data. The LBL/GSI/ANL streamer chamber collaboration has painstakingly reconstructed 162 complete events for the ^{40}Ar + KCl system at 1.8 GeV/amu. An automatic measuring system being developed will permit better statistics in the future. Meanwhile, this sample of events has permitted development of analysis techniques for 4π data and some early conclusions as discussed below.

To analyze 4π data we first try the simplest global variables, such as sphericity. The sphericity tensor is defined for each event in momentum space:

$$S_{ij} = \sum_{\nu=1}^{n} P_{i\nu} P_{j\nu}$$

where the sum runs over all the particles in that event. For heavy ion collisions at relatively low energies it is useful to introduce a weighting according to the particle mass, giving the energy flow tensor:

$$F_{ij} = \sum_{\nu=1}^{n} P_{i\nu} P_{j\nu}/2m$$

This tensor, introduced by Gyulassy, Frankel and Stocker[13], has specifically the advantage that it deals appropriately with composite particles in the context of coalescence. Without the mass weighting a deuteron would contribute twice as much as the nucleons it contains would if counted separately.

Figure 16 shows how this variable distinguishes models in terms of the shape of the energy flow tensor. The insert shows a cross cut on the event in momentum space. The longest and shortest axes of the energy flow ellipse are chosen to fall in the plane of the paper. The location of an event in the flow ratio vs flow angle plot indicates the shape and orientation of the ellipse as shown around the margin. The two curves are for two models, cascade[14] and hydrodynamical flow[13]. The points represent events with impact parameters b where 10 b/b_{max} is used as a label. The cascade predictions also include a statistical straggle around the points plotted, but the hydrodynamical calculations do not yet include fluctuations.

The comparison between theory and experiment is most easily made for cascade models since detector efficiencies can very easily be incorporated into the theory. Figure 17 shows schematically how this is done. Figure 18 shows the results of such a comparison for the 162 events so far measured in 1.8 GeV/amu ^{40}Ar + KCl collisions with a central trigger. It is clear that the data include events with more elongated energy flow ellipsoids and with larger flow angles than do the cascade calculations. This supports the inclusion of coherent effects, which are not present in the cascade model.

The streamer chamber is presently being upgraded to a hybrid system with a 400-element scintillator array to provide advanced triggering capabilities and improved particle identificaton.

2e. Exclusive Charged Particle Measurements: HISS

Another major detector just completed at the Bevalac is the Heavy Ion Superconducting Spectrometer (HISS). This has a large array of detectors under construction as shown in Figure 19. The drift chamber module defines particle trajectories; the time-of-flight walls give Z,A identification for A < 12. The multiple sampling ionization chamber (MUSIC) provides Z identification up to Z = 92.

A subset of these detectors has been used for preliminary measurements in the projectile fragmentation region. Various charged-particle fragmentation modes of ^{12}C were studied, with effective mass reconstruction within a few MeV. After integrating over all the solid angle in the fragmentation region, relative fragmentation probabilities could be obtained, as shown in Figure 20. Such results will shed light not only on the fragmentation mechanism but also on the internal structure of the nuclei involved.

3. Anomalous Projectile Fragments (Anomalons)

In the study of the projectile fragmentation region over the years, starting with cosmic rays, it has been observed that projectile fragments of a given charge Z did not interact in emulsion in the same way as normal nuclei of the same charge. It is only recently, as a result of Bevalac experiments, that the statistical significance of such results has become convincing. At this time the subject is both extremely exciting and controversial.

In a typical experiment an emulsion stack is exposed to a beam of primary nuclei and the interactions of the primary nuclei are studied as a function of distance into the stack. An exponential absorption is found, the slope of which gives the mean free path. Figure 21 shows the mean free path for ^{16}O primary nuclei as extracted from interactions taking place at various distances from entry into the emulsion. The constancy of the mean free path is consistent with the expected exponential absorption.

On the other hand, if instead of studying primary nuclei we observe secondary nuclei produced in the projectile fragmentation region, we find a deviation from exponential absorption: the mean free path is shorter than expected in the first cm or so after the production point of the secondary nucleus. To combine results from secondary nuclei of various charges, Friedlander et al.[15] have used a scaling formula, which enables them to show, as in Figure 22, the combined ratio of observed mean free path to expected mean free path as a function of distance. They fit the data by assuming that 6% of the fragments have an unusually short mean free path, 2.5 cm. These 6% are called "anomalons".

Figure 23 shows combined results from three experiments, that of ref. 15, an independent experiment by Jain et al.[16], and a cosmic-ray experiment carried out over many years by Barber et al.[17] All the results are consistent with normal mean free paths at distances greater than 2-4 cm from production, with an enhanced probability of interaction at shorter distances. In the following I will summarize what is known, or believed to be known, about this phenomenon.

(a) Existence: The evidence for the phenomenon is at the 3-5 s.d. level, depending on whether an individual experiment is taken or the total of all observations. Criticism of the observations has mainly revolved about statistical analysis methods and finite thickness effects in the emulsion stacks, about the scaling procedure involved in combining all secondary fragments into a common data set, and about a variety of possible scanning biases especially related to efficiency for detecting interactions of various kinds.

The question of statistical methods is readily disposed of since extensive Monte Carlo simulations of the phenomenon have shown that the methods used are free of systematic bias. As usual, the level of significance one can quote for the effect depends on which statistic is chosen to test for it, and the uncertainty is also uncertain. Such effects are not, however, peculiar to this phenomenon.

The question of scaling parametrization is more difficult. The scaling formulae are based on a simple Z-dependence fitted to measurements made at the Bevalac for primary nuclei. Scaling

according to Z obviously fails badly for very light nuclei (e.g., p, d, t, ^{3}He, ^{4}He) so the data for low charges are very suspect. The data shown in Figures 22,23 are for $Z \geqslant 3$. For heavier nuclei, plausible models for the dependence of mean free path on neutron or proton excess do not give sufficient variation to account for the data.

Various systematic biases have been postulated, depending mainly on the fact that interactions in emulsion vary from very mild non-charge-changing interactions that cannot be detected at all to dramatic stars with many secondary particles. Interaction cross sections measured in emulsion therefore depend on scanning instructions and are always substantially lower than calculated reaction cross sections. This should not affect the observations provided that uniform criteria are employed and that scanning efficiency is constant and known. Internal checks on the data indicate that scanning efficiency is very high where it matters, and tests that it does not depend on distance from the primary interaction give satisfactory results, albeit with a lower level of significance than the overall effect.

It therefore seems that the effect is real, though much higher statistical accuracy would be very desirable to be convincing and to provide for the many cross-checks that are desirable.

(b) Lifetime: On any scale of expectations the lifetime of the anomalons is very long. Since they live at least a cm or so before decay or interaction, their lifetime in their rest frame must be more than about 10^{-11} s. They thus have sharp mass, which could be measured in an appropriately designed experiment.

(c) Interaction Cross Section: The effect is identified in the existing data by a roughly 20% enhancement in the interaction cross section measured in the first few cm after production. Two interpretations of this are equally acceptable: Friedlander et al.[15] postulate that the anomalons are relatively stable, constitute a 6% component of the yield, and have roughly ten times enhanced interaction cross sections. Alternatively, the observation would be explained if <u>all</u> the secondary fragments have a 20% enhanced cross section on production but decay by neutral particle (or photon) emission to normality with a lifetime of about 10^{-11} s.

Which assumption is more dramatic depends on taste. "Conventional" explanations usually address the latter since a 20% enhancement of cross section is at least thinkable in nuclear physics. However, no adequate explanation has surfaced. Explanations involving excitation of quark-gluon degrees of freedom usually prefer the former because the 6% probability of exciting such a state seems a hard enough objective, let alone 100%.

(d) Persistence of Anomalous Property: Friedlander et al.[15] reported that there is a correlation between short-range secondary interactions and short-range tertiary interactions. The statistical evidence for this is at about a 3 s.d. level based on a smaller sample of events. If this result is correct it puts major constraints on any possible explanation of the phenomenon.

(e) Integral Charge: Judek[18,19], who is responsible for the overwhelming body of information concerning anomalons, remarks that the anomalous fragments have integral charge, but does not display the data. Figures 24,25 show preliminary data on fragments of charge 1,2,3 in emulsion and 12 to 18 in plastic track detector CR 39. While the statistics are poor and the fragments have not been sorted according to their interaction points, it is clear that charge resolution can be very good and that no evidence for fractional charge is obvious.

(f) Universality of Effect: Most of the data are for fragments of charge $Z \geqslant 3$, and within those data the evidence seems not to be focused on any particular charge region. The effect therefore seems to have some kind of universal character. Judek[19] has reported evidence for a strong effect in charges 1,2 in a very detailed paper. As remarked before, data for charge 1 should be specially sensitive to an isotope effect, and there are known to be many deuterons and tritons in the projectile fragmentation region. However, the presence of these particles would be expected to lower the <u>average</u> mean free path, not to produce the very short 1-2 cm phenomenon observed. Judek reports an effect for charge 2. Recent high statistics measurements have been made for charge 2, but the preliminary results are rather confusing.

The observation of the effect in very light nuclei would potentially be of capital importance because any explanation

involving complex nuclear energy levels would not be possible.

(g) Transverse Momentum Dependence: Judek[19] reports that the effect is maximized at transverse momenta of 200-500 MeV/c.

(h) Production Threshold: There is fragmentary evidence that the production may drop below about 1 GeV/amu primary energy and above about 5 GeV/amu, but it is not strong[19,20]. It would be specially valuable to study the effect as a function of energy since the variation of the Lorentz factor should indicate clearly if there is a decay phenomenon involved.

(i) Topological Differences in the Interactions: Here we have anecdotal information that there is no startling difference between the stars produced at short and at long distances from the fragment production point. Judek[19] does report that the shortest mean free paths are seen for interactions with $N_h = 0$, i.e., interactions with hydrogen in the emulsion. She also remarks that the topology of the stars is such as to rule out hypernucleus decay.

3a. Experiments in Progress

The above observations point to some follow-up experiments that are being carried out in addition to improvement of the emulsion measurements by accumulation of improved statistics and other systematic studies.

(a) Search for Decay Photons: If the anomalons decay downstream from the production target, the decay products might be high energy photons. Price et al. have conducted a study to look for photons above about 30 MeV detected in a Pb-glass array collimated to look, in vacuo, 1.4 to 2.7 cm downstream from a target. In the preliminary analysis of the results, this type of decay seems to be ruled out.

(b) Search for Decay Charged Particles: Assuming that the anomalons have a fairly long lifetime but finally decay, the HISS spectrometer could, under favorable circumstances, reconstruct the decay vertex and measure the effective mass, which should be sharp. Greiner has described this experiment at the GSI Workshop in 1980[21]. The necessary vacuum system has now been constructed and results should be available soon.

(c) Search for Anomalous Target Fragments: Arguing that anomalons should occur among the target fragments, if projectile and target

are interchanged, Koontz et al[22] have looked for charge-1 anomalons, following the emulsion work of Judek[19]. The anomalons would be seen in the momentum range 200-500 MeV/c under a variety of circumstances--if they entered the solid-state detectors for direct observation, if they emitted photons in the 100-400 MeV region at a sharp energy, or if they emitted charged particles and photons in coincidence. This experiment has been run and is undergoing analysis.

(d) Target Density Effect: The Poskanzer-Gutbrod group is planning to conduct an experiment using the Plastic Wall to look for an effect due to target density, which would distinguish between decay and absorption as a reason for the apparent disappearance of the anomalons 1-2 cm after production. The Plastic Wall is used as a detector for the total spectrum of Z^2 of the produced fragments, primary, secondary, tertiary, etc. The decay hypothesis should lead to a difference between the spectrum observed for a dense and dilute target of the same thickness.

(e) Plastic Track Detectors: Price et al. at Berkeley and Heinrichs et al. at Siegen have exposed plastic track detectors to ^{40}Ar beams from the Bevalac. These are sensitive to the higher-Z fragments and have excellent charge resolution (see Fig. 25). In particular, the Siegen group has a fully automatic measuring procedure that will lead to excellent statistics. At this meeting, Heinrichs announced that preliminary data are becoming available in which about 20,000 fragments have been measured with $Z > 8$ and special emphasis is being placed on 5923 fragments with $Z = 14$. It is clear that inadequate statistics will no longer be a problem and that by concentrating on a particular value of Z, scaling assumptions will not be needed to such an extent in analyzing the data.

4. Future Experiments

The Bevalac has just been upgraded to provide uranium capability. During the Bielefeld meeting success was achieved and the first (1000 particles per pulse) beam was extracted. In the next year or so the intensity will be raised to 10^7-10^8 per pulse. Emulsion exposures show typical cone-shaped tracks, many

fission type events, and some more central collisions. The next years at the Bevalac will provide the first opportunity to study equilibration properties of really large nuclear systems in the relativistic region.

5. Acknowledgments

I am indebted to S. Nagamiya, M. Gyulassy, W.A. Zajc, H.H. Gutbrod, A.M. Poskanzer, J.W. Harris, D.E. Greiner, H.H. Heckman, and P.B. Price for unpublished material and for discussions concerning the preparation of this talk. I am also indebted to all the other Bevalac enthusiasts who will forgive me for not discussing their activities.

This work was supported by the Director, Office of Energy Research, Division of Nuclear Physics of the Office of High Energy and Nuclear Physics of the U.S. Department of Energy under Contract DE-AC03-76SF00098.

6. References

1. S. Nagamiya, et al., Phys. Rev. C24, 971 (1981)
2. S. Schnetzer, Thesis, LBL-13727 (1981)
3. H. Stöcker, A.A. Ogloblin and W. Greiner, LBL-12971 (1981)
4. S. Nagamiya and M. Gyulassy, LBL-14035 (1982), to be published in Advances in Nuclear Physics
5. J.W. Harris, et al., Phys. Rev. Lett. 47, 229 (1981)
6. P. Koch, J. Rafelski and W. Greiner, Univ. of Frankfurt Theoretical Preprint UFTP-82-77 (1982)
7. A. Shor, et al., LBL-14229 (1982)
8. S.Y. Fung, et al., Phys. Rev. Lett. 41, 1592 (1978)
9. W.A. Zajc, et al., Proc. 5th High Energy Heavy Ion Summer Study, ed. L.S. Schroeder, LBL-12652 (1981) p. 350
10. M. Gyulassy, Phys. Rev. Lett. 48, 454 (1982)
11. J.J. Lu, et al., Phys. Rev. Lett. 46, 898 (1981)
12. H. Stöcker, J.A. Maruhn and W. Greiner, Phys. Rev. Lett. 44, 725 (1980)
13. M. Gyulassy, K.A. Frankel and H. Stöcker, Phys. Lett. 110B, 185 (1982)
14. J. Cugnon, Phys. Rev. C22, 1885 (1980)
15. E.M. Friedlander, et al., Phys. Rev. Lett. 45, 1084 (1980)
16. P.L. Jain and G. Das, Phys. Rev. Lett. 48, 305 (1982)
17. H.B. Barber, P.S. Freier and C.J. Waddington, Phys. Rev. Lett. 48, 856 (1982)
18. B. Judek, Can. J. Phys. 46, 343 (1968)
19. B. Judek, Can. J. Phys. 50, 2082 (1972)
20. M.M. Aggarwal, et al., Phys. Lett. 112B, 31 (1982)

21. D.E. Greiner, Proc. Workshop on Future Relativistic Heavy Ion Experiments, GSI Darmstadt, 1980, ed. R. Bock, R. Stock, GSI 81-6, p. 470 (1981)
22. R.W. Koontz, et al., Bevalac Proposal 630H

7. Figure Captions

1. A streamer chamber photograph of an ^{40}Ar + Pb collision at 1.8 GeV/amu, courtesy S.Y. Fung, et al.
2. Schematic illustration of a relativistic heavy ion collision in the sudden approximation, with subsequent explosion of the participant region.
3. Proton inclusive energy spectra for several systems at θ_{cm} = 90° and 800 MeV/amu, from reference 1.
4. Pion inclusive energy spectra at θ_{cm} = 90° and several energies, for Ne + NaF collisions, from reference 1.
5. K^+ inclusive energy spectra for Ne + NaF at 2.1 GeV/amu, combined data from several angles. Data from references 1,2.
6. Inverse slope parameters for Ne + NaF at θ_{cm} = 90°. Data from reference 4.
7. Schematic time development of a heavy ion collision showing emission times of various observed particles, courtesy S. Nagamiya.
8. Two pion intensity interferometry measurements, from reference 9.
9. Radius parameter extracted by Lu, et al. (reference 11) by pion intensity interferometry for ^{40}Ar + KCl at 1.8 GeV/amu.
10. Hydrodynamic bounce-off effect predicted at large impact parameters. Figure taken from ref. 12.
11. Schematic picture of the Plastic Ball-Wall layout.
12. One element of the Plastic Ball.
13. Particle discrimination in the Plastic Ball.
14. Deuteron to proton ratio observed as a function of total charged particle multiplicity in the Plastic Ball/Wall.
15. Coalescence in the C + C system at 0.8 GeV/A, from reference 1.
16. Calculated energy flow diagram for U + U at 400 MeV/amu. For detailed discussion see reference 13.
17. Schematic analysis procedure for comparison between theory and experiment using the Plastic Ball or Streamer Chamber.
18. Energy flow diagrams similar to Figure 16 but with real data from the ^{40}Ar + KCl system at 1.8 GeV/amu (18a) and simulated data from a cascade model (18b).
19. The layout of the HISS spectrometer and its detectors. Several trajectories of beam velocity particles are shown, as well as one for lower energy protons.
20. Preliminary yields of various production channels in ^{12}C fragmentation at 1.9 GeV/amu. Measurement with HISS, private communication, D.E. Greiner.
21. Mean free path extracted for ^{16}O nuclei in emulsion, data from H.H. Heckman, private communication.
22. Anomalous mean free path effect; data from reference 15.
23. Anomalous mean free path effect; combined data from references 15,16,17.
24. Charge resolution achieved for particles of charges 1,2,3 in emulsion; private communication, H.H. Heckman.
25. Charge resolution achieved for particles with Z = 12-18 in plastic track detector CR 39; private communication P.B. Price.

Table I
Two pion interferometry data for ^{40}Ar + KCl
at 1.8 GeV/amu from reference 9

	λ	R(fm)	χ^2/d.f.
$2\pi^-$, raw	$\equiv 1$	1.84 ± 0.27	114/113
$2\pi^-$, Coulomb corrected	$\equiv 1$	2.98 ± 0.30	120/113
$2\pi^-$, "	0.86 ± 0.07	3.12 ± 0.33	116/113
$2\pi^+$, "	0.78 ± 0.07	3.92 ± 0.43	89/109

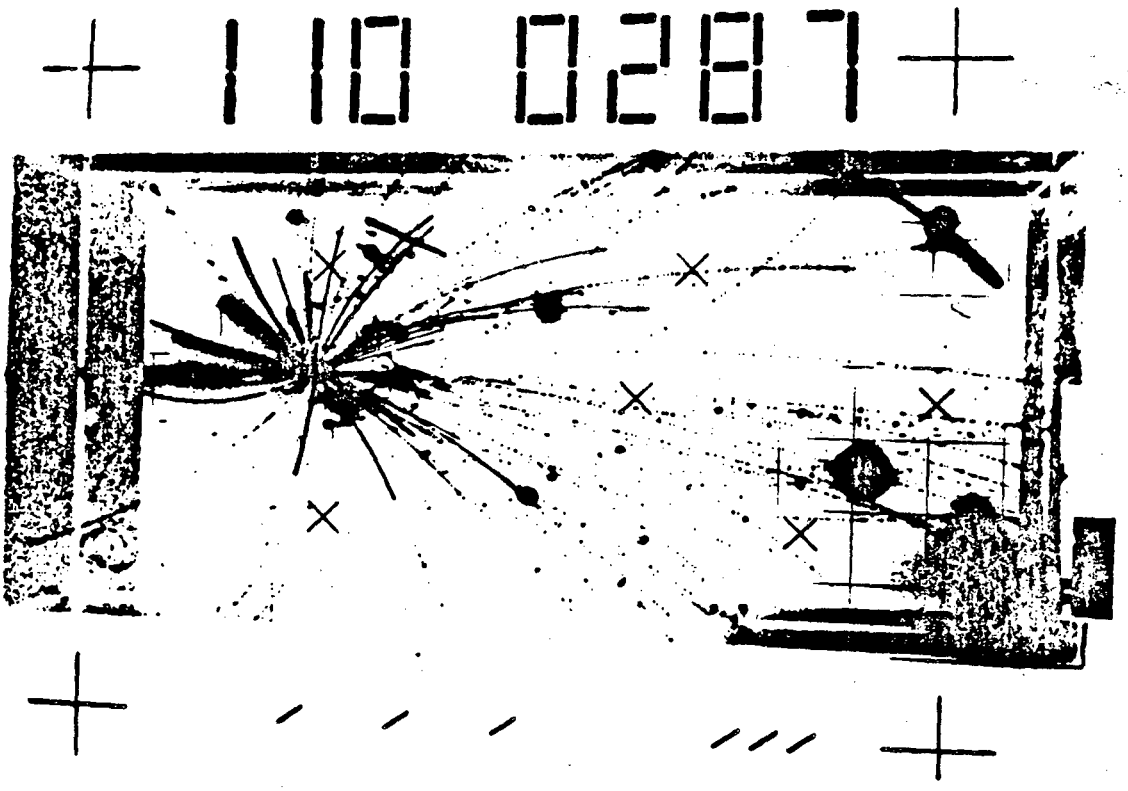

Figure 1

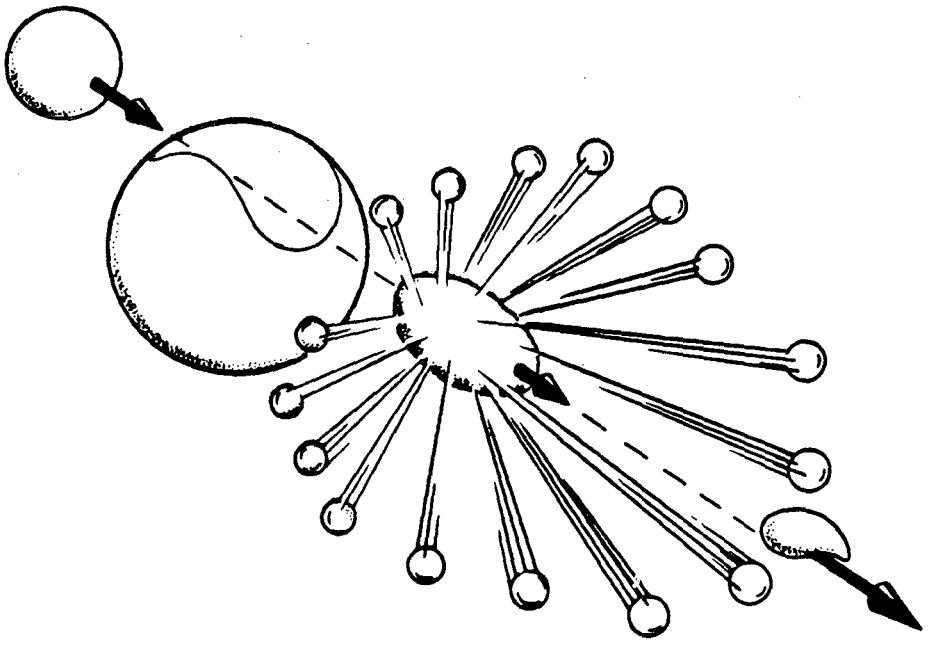

Figure 2

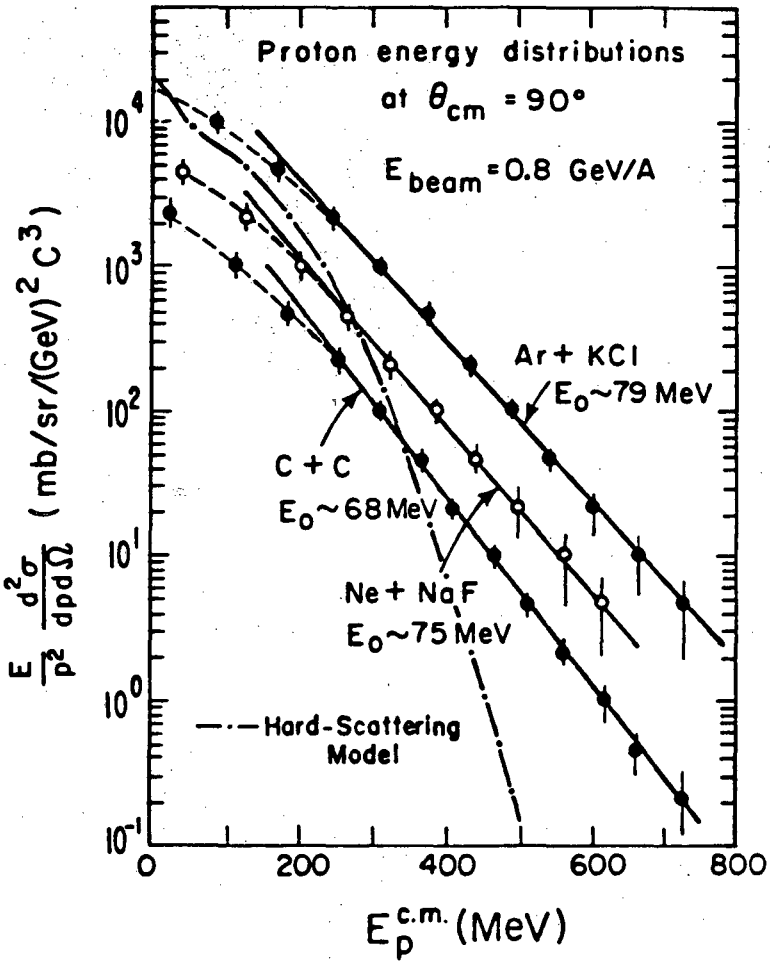

Figure 3

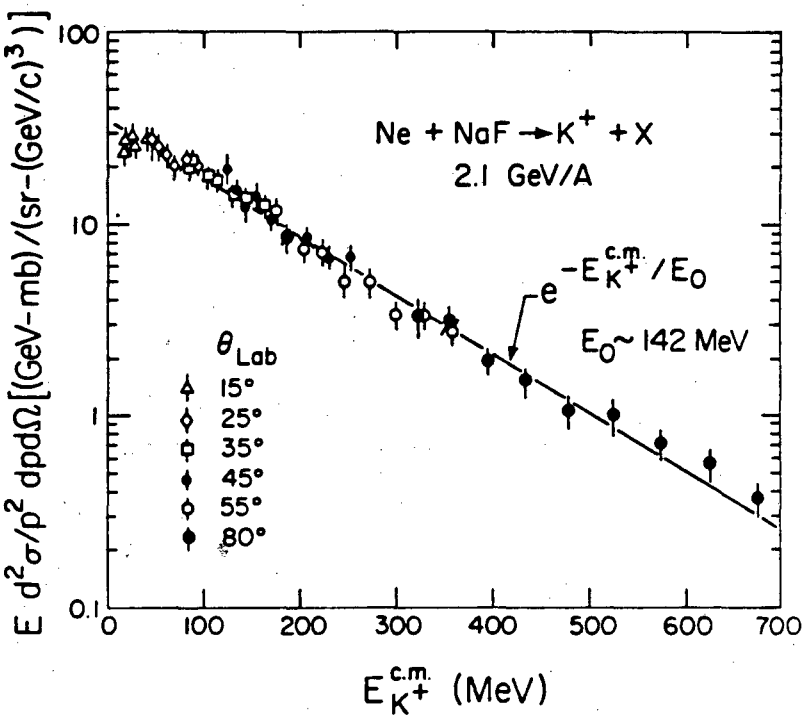

Figure 5

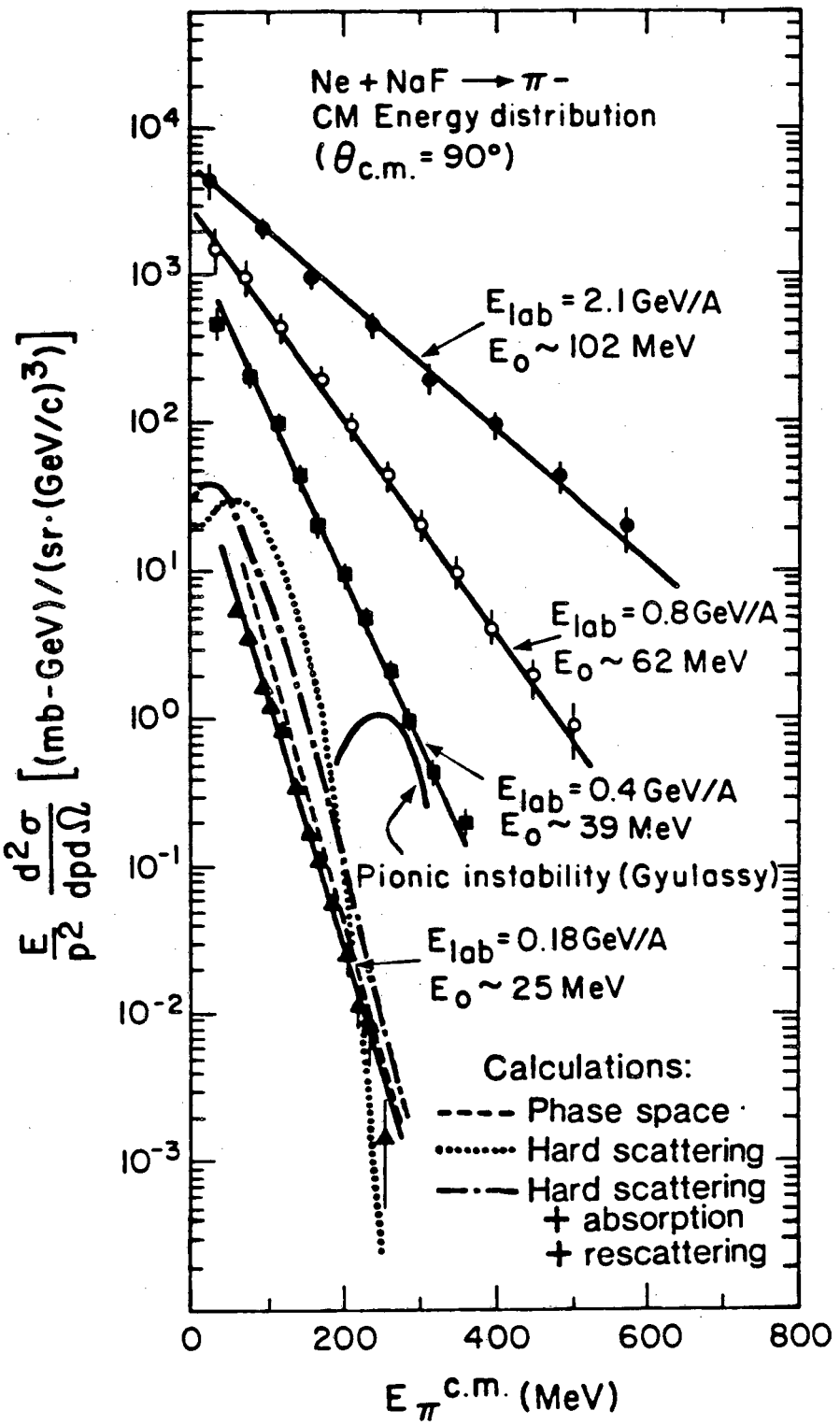
Ne + NaF → π⁻
CM Energy distribution
(θc.m. = 90°)
Elab = 2.1 GeV/A
E0 ~ 102 MeV
Elab = 0.8 GeV/A
E0 ~ 62 MeV
Elab = 0.4 GeV/A
E0 ~ 39 MeV
Pionic instability (Gyulassy)
Elab = 0.18 GeV/A
E0 ~ 25 MeV
Calculations:
Phase space
Hard scattering
Hard scattering + absorption + rescattering
E d²σ/p² dpdΩ [(mb-GeV)/(sr·(GeV/c)³)]
Eπ c.m. (MeV)
10⁴
10³
10²
10¹
10⁰
10⁻¹
10⁻²
10⁻³
0
200
400
600
800

Figure 4

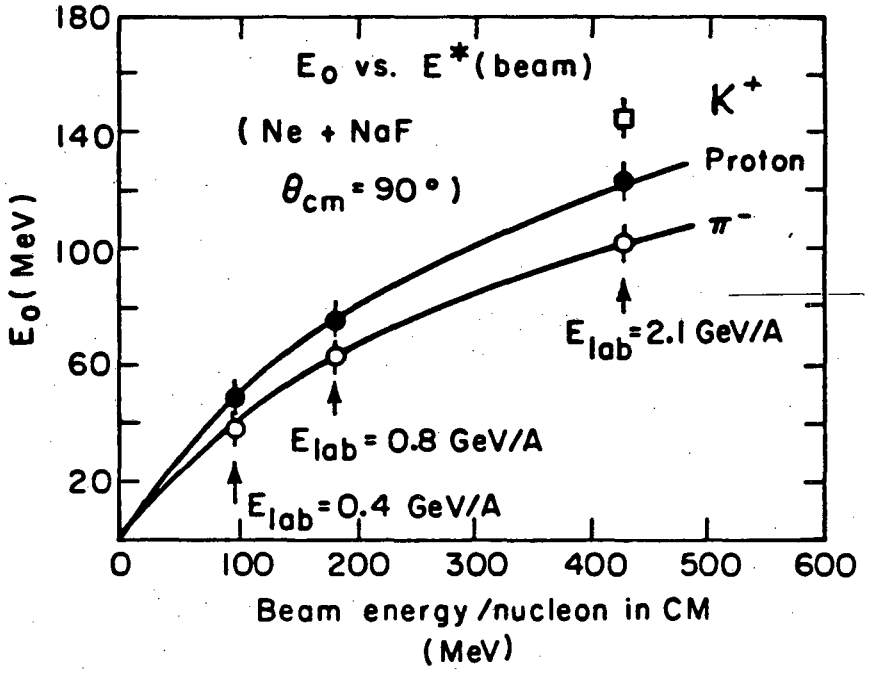

Figure 6

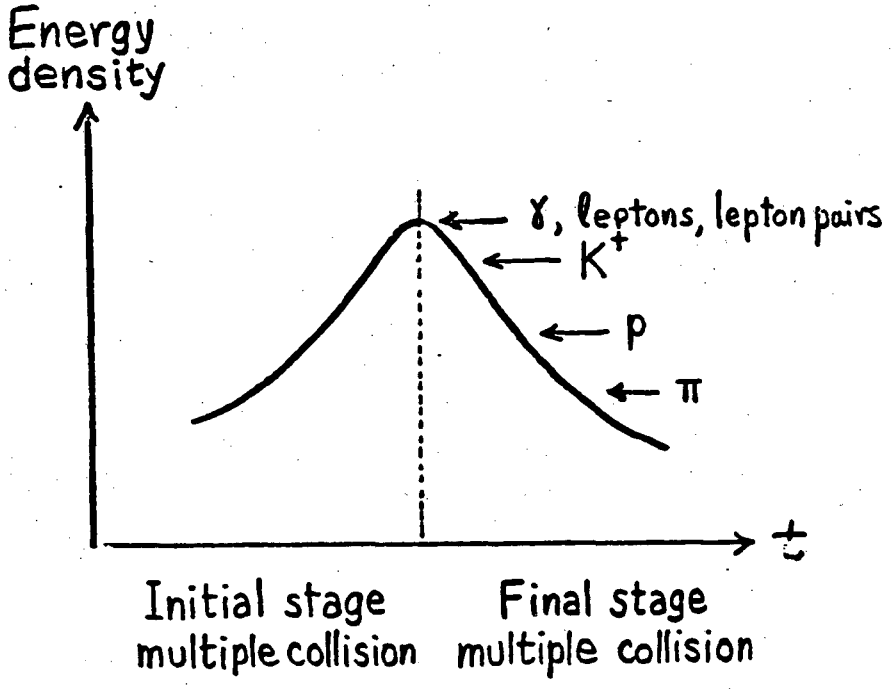

Figure 7

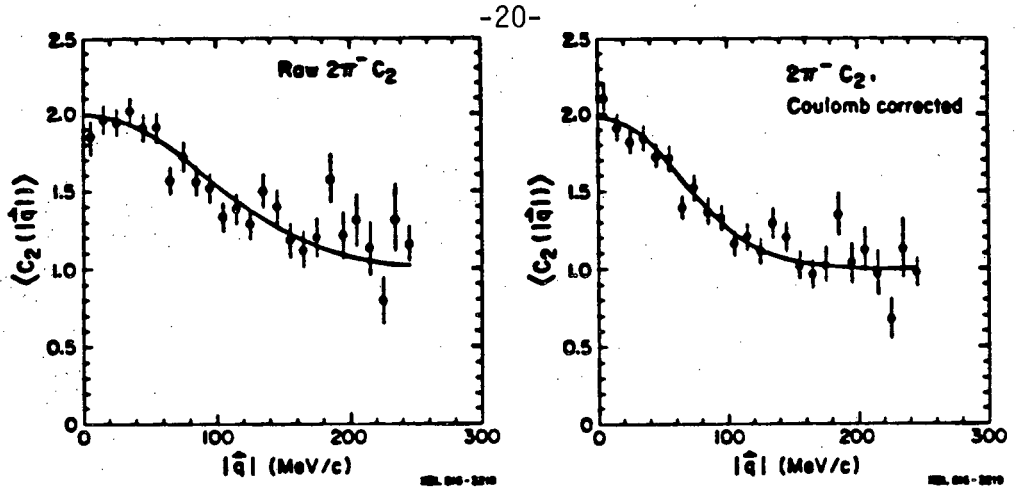
Raw $2\pi^- C_2$
$2\pi^- C_2$, Coulomb corrected
$\langle C_2(|\hat{q}|)\rangle$
$|\hat{q}|$ (MeV/c)
0
0.5
1.0
1.5
2.0
2.5
100
200
300

a.) b.)

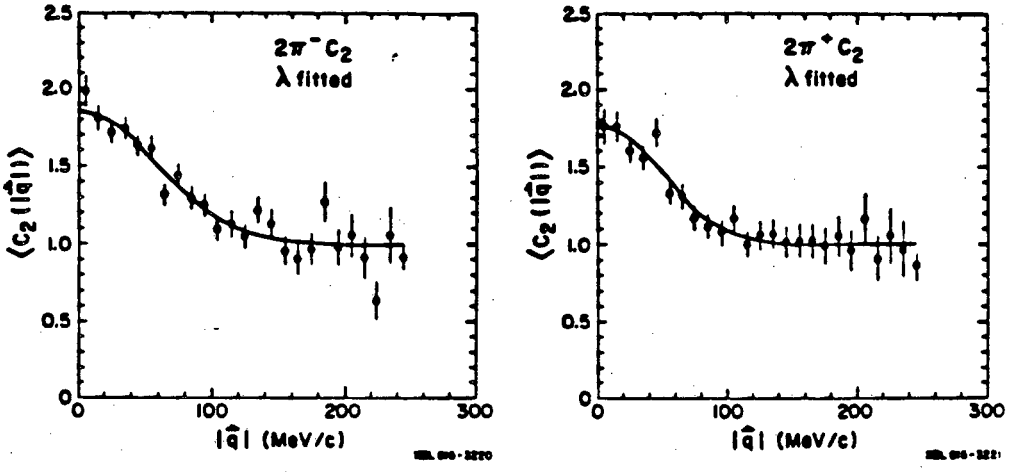
$2\pi^- C_2$ λ fitted
$2\pi^+ C_2$ λ fitted
$\langle C_2(|\hat{q}|)\rangle$
$|\hat{q}|$ (MeV/c)
0
0.5
1.0
1.5
2.0
2.5
100
200
300

c.) d.)

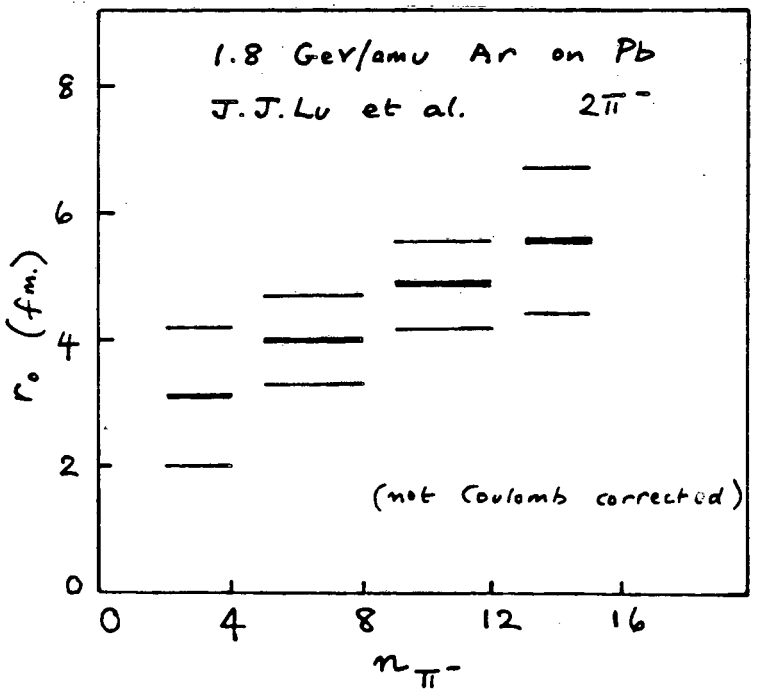
1.8 GeV/amu Ar on Pb
J. J. Lu et al. $2\pi^-$
(not Coulomb corrected)
r_o (fm.)
n_{π^-}
0
2
4
6
8
0
4
8
12
16

Figs. 8,9

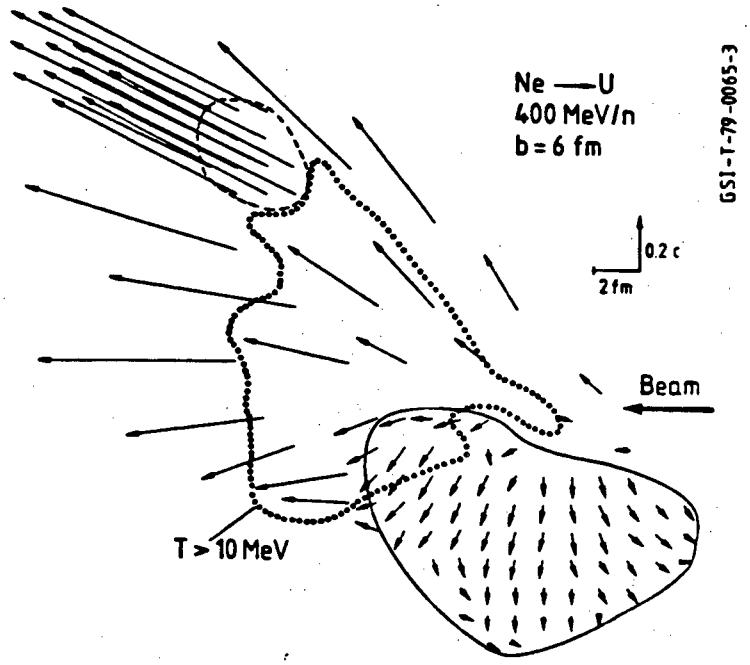

Figure 10

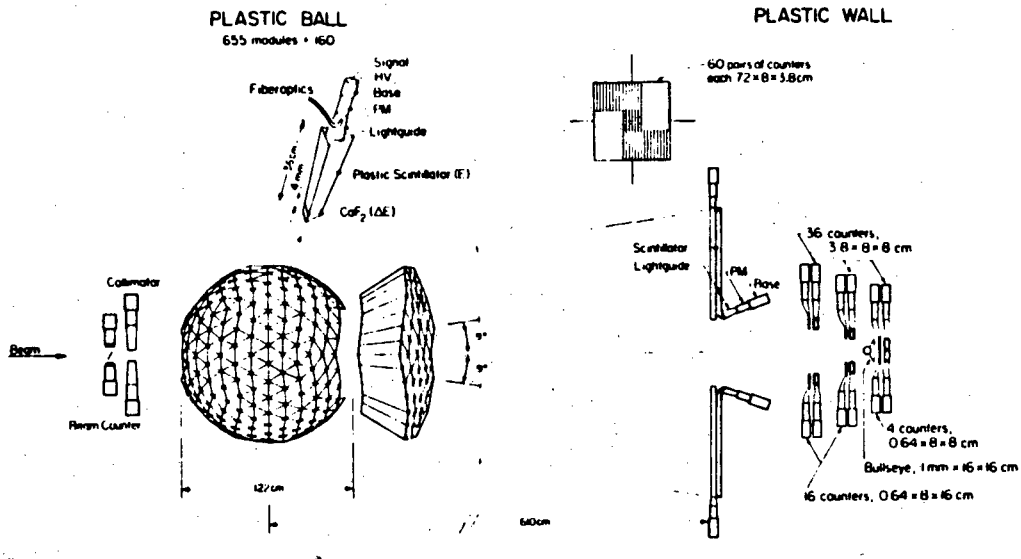

Figure 11

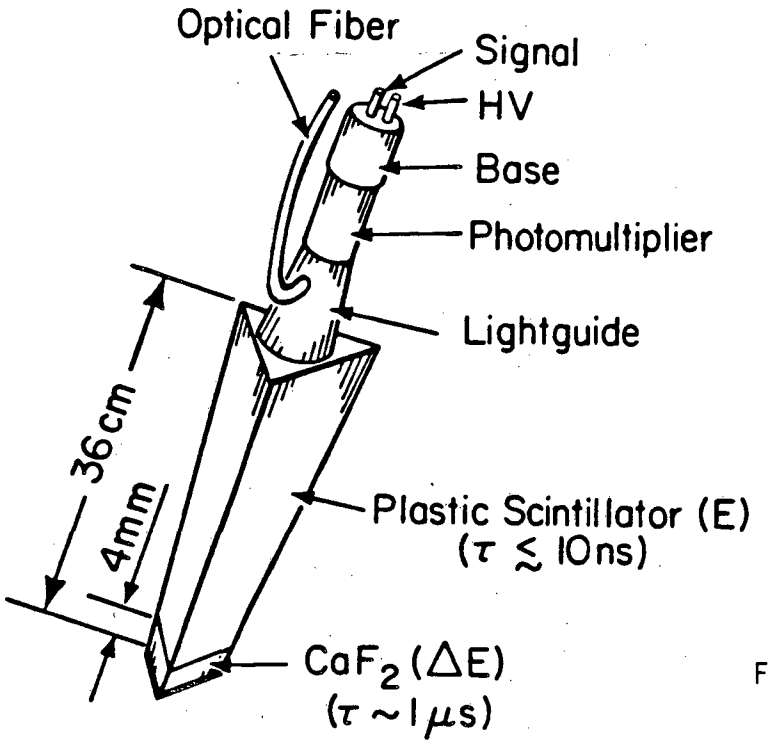

Fig. 12

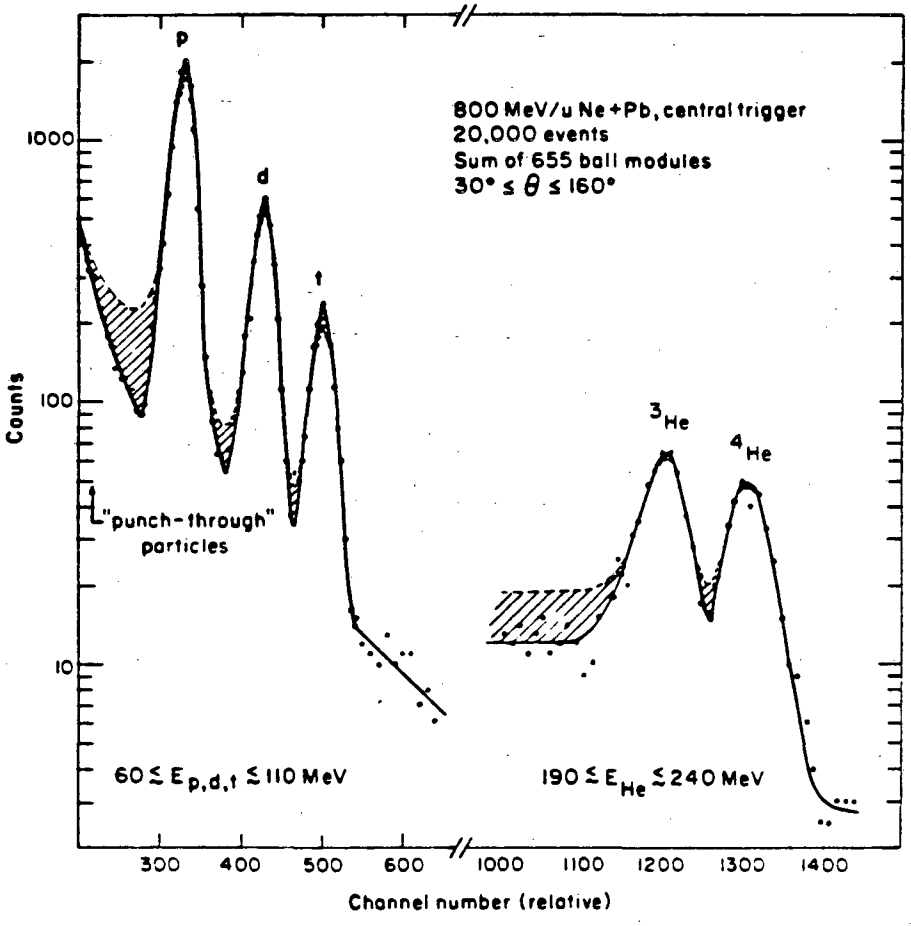

Figure 13

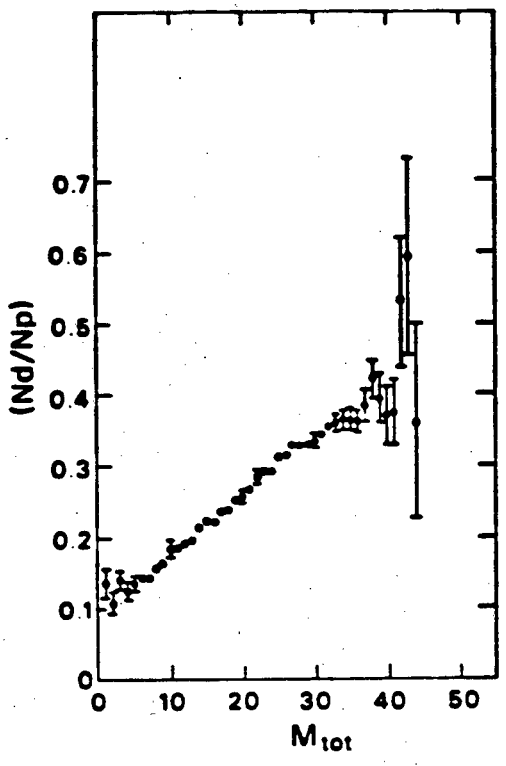

Fig. 14

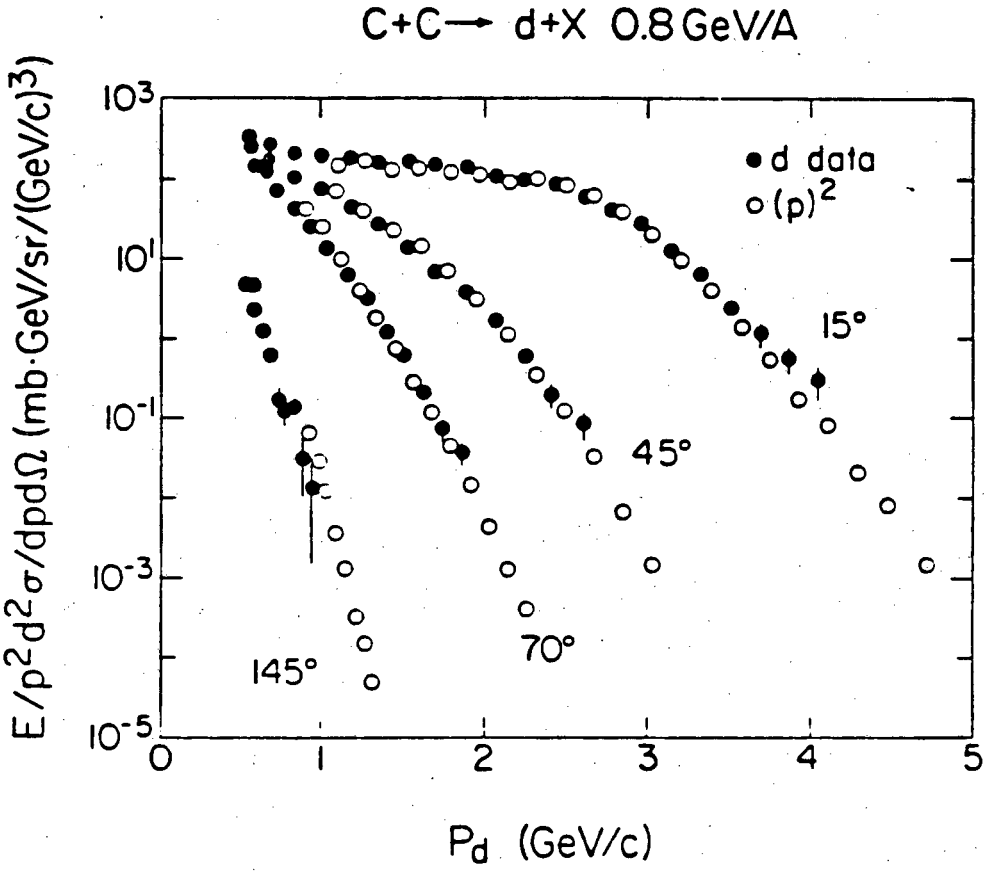

Figure 15

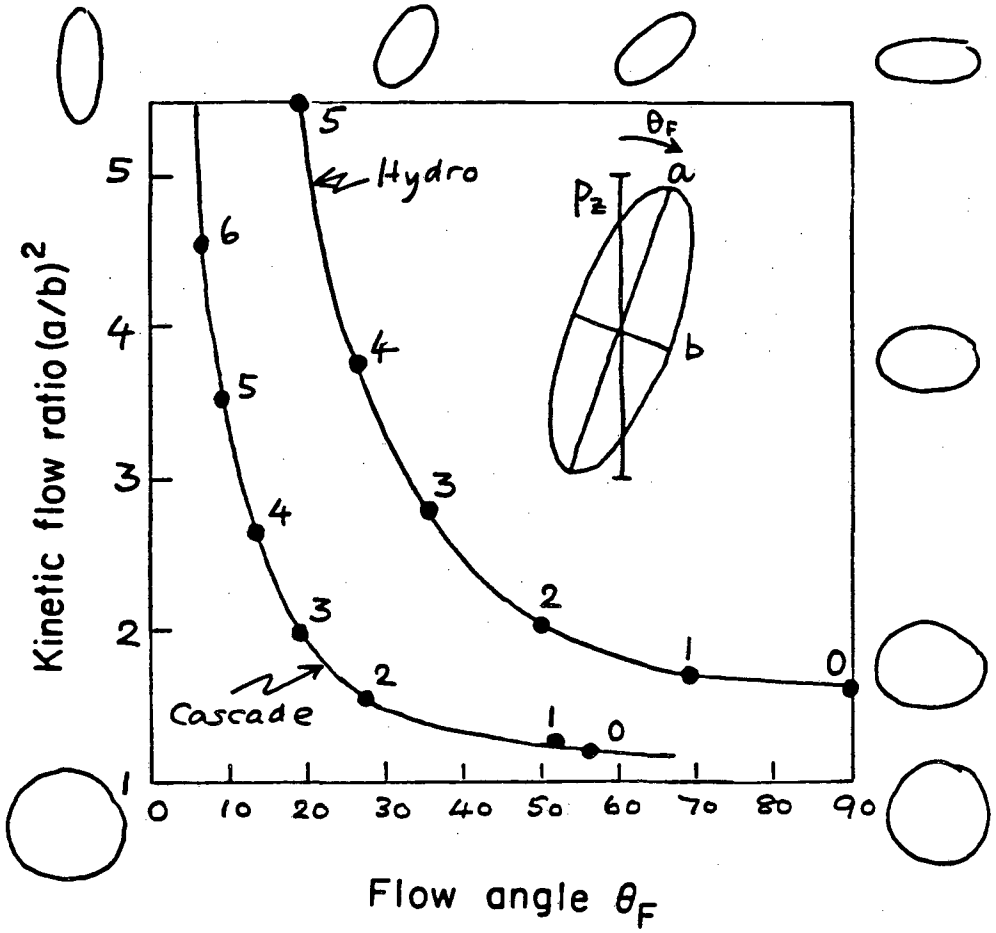

Figure 16

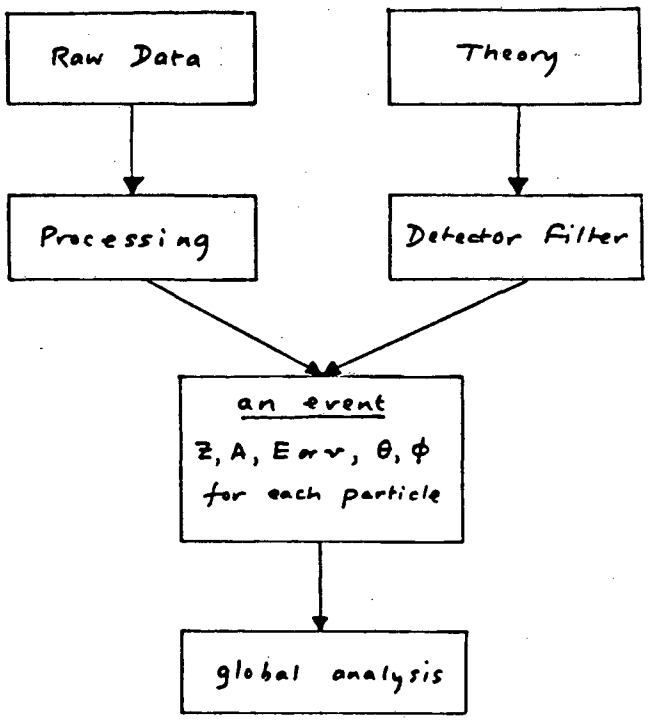

Fig. 17

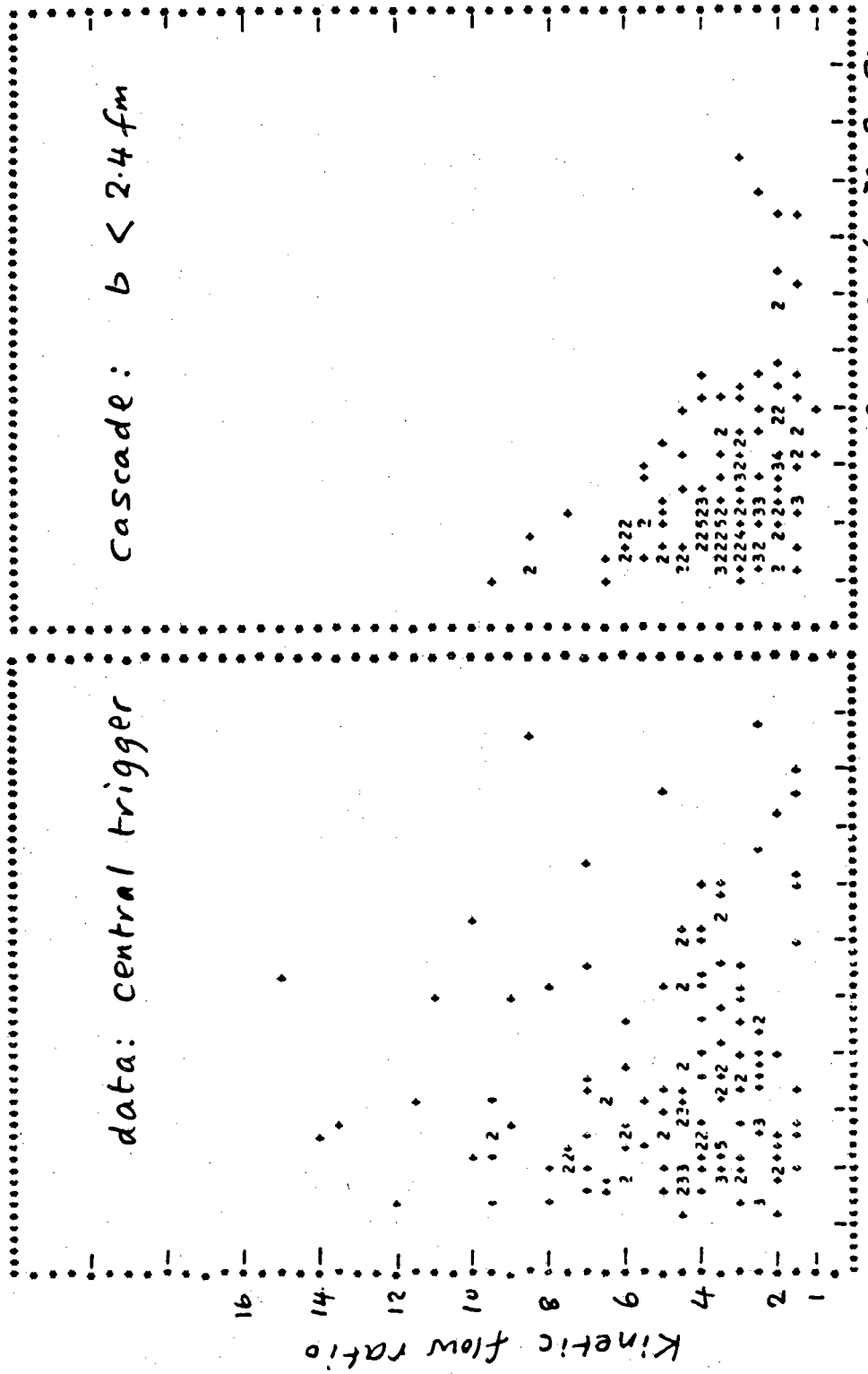
data: central trigger
Cascade: b < 2.4 fm
Kinetic flow ratio
flow angle (degrees)

Figure 18

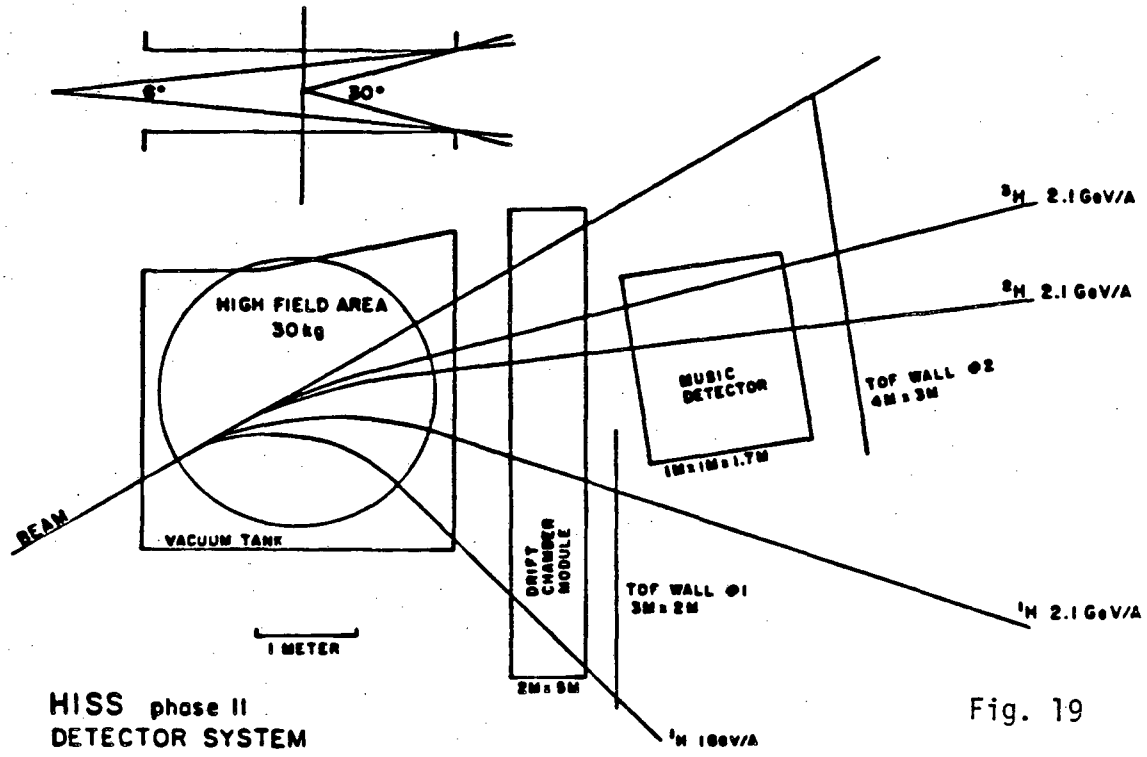

HISS phase II
DETECTOR SYSTEM

Fig. 19

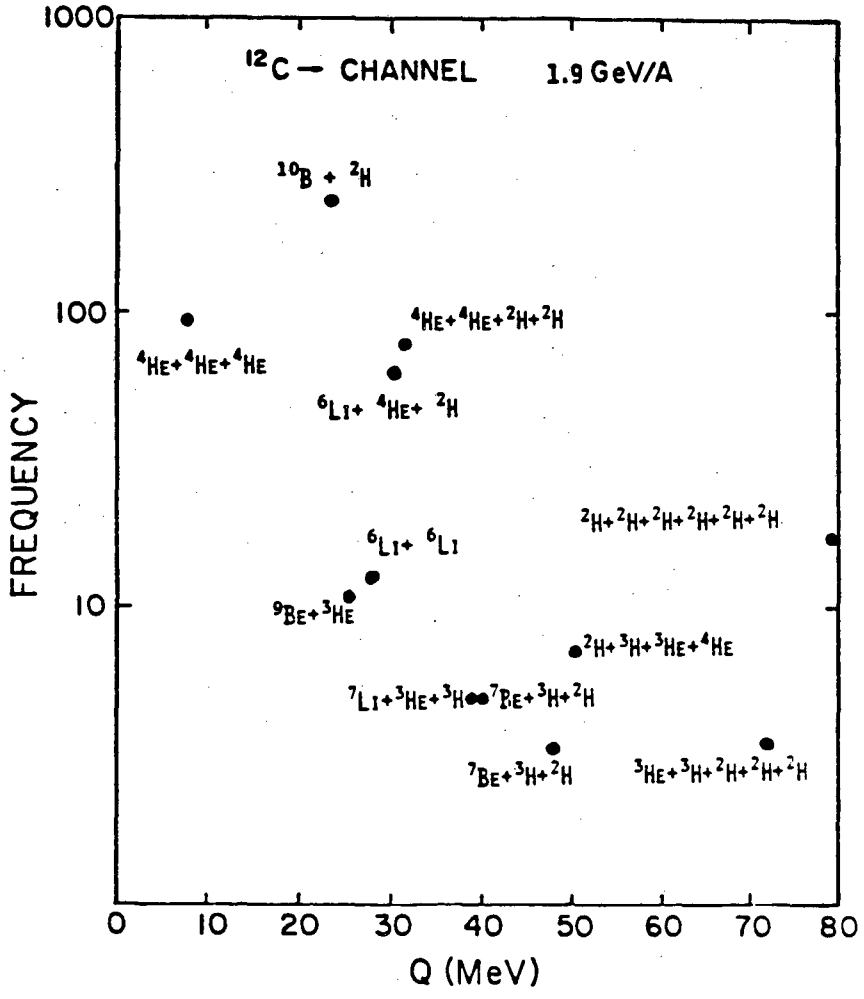

Fig. 20

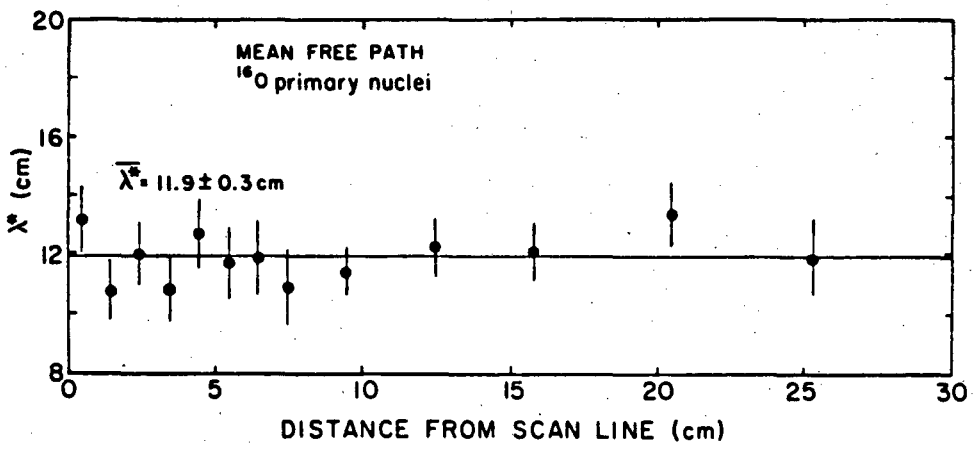

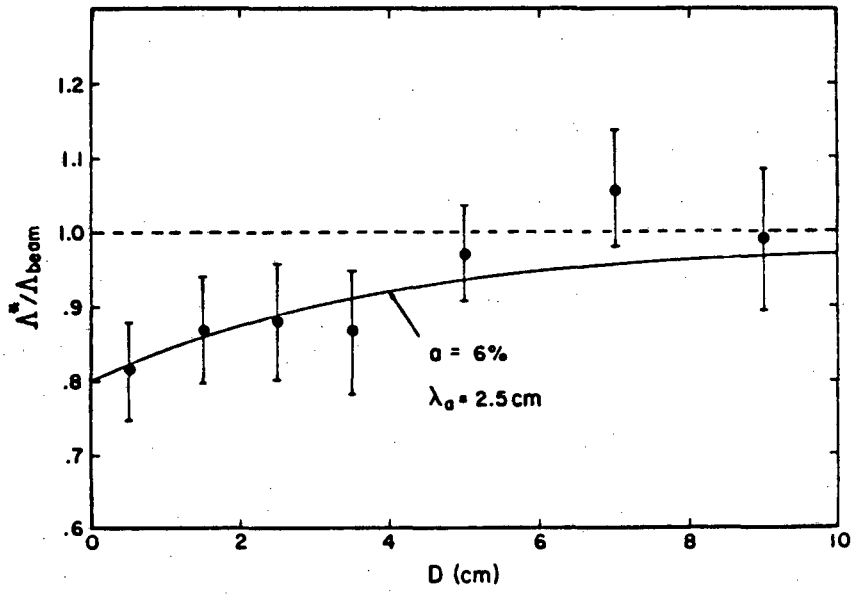

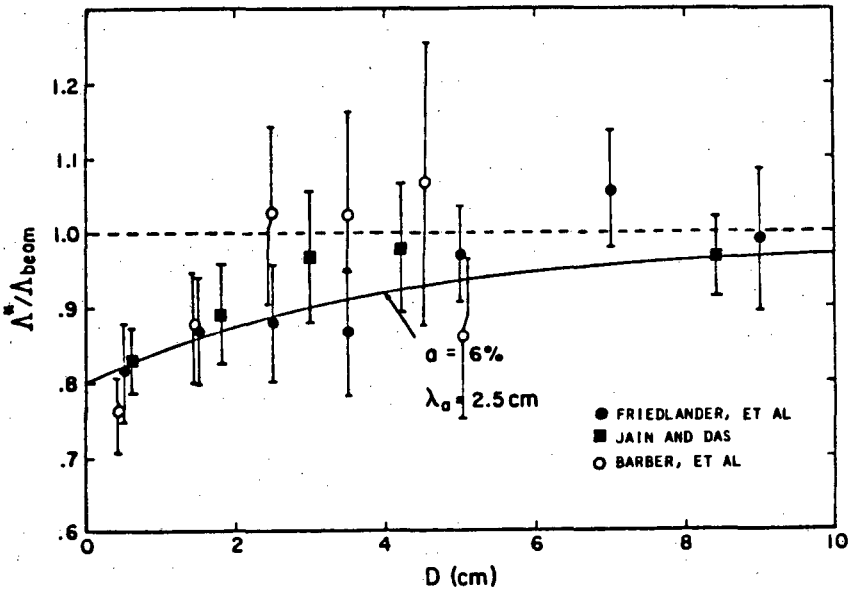

Figures 21 (top), 22, 23 (bottom)

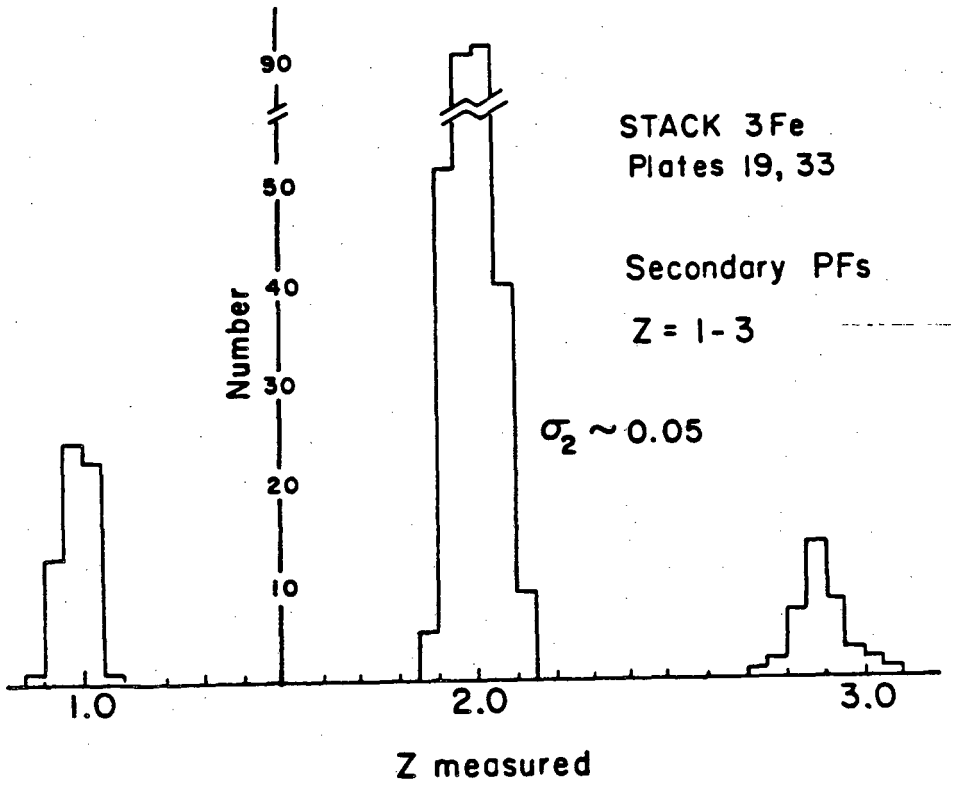
STACK 3Fe
Plates 19, 33
Secondary PFs
Z = 1-3
$\sigma_2 \sim 0.05$
Number
90
50
40
30
20
10
1.0
2.0
3.0
Z measured

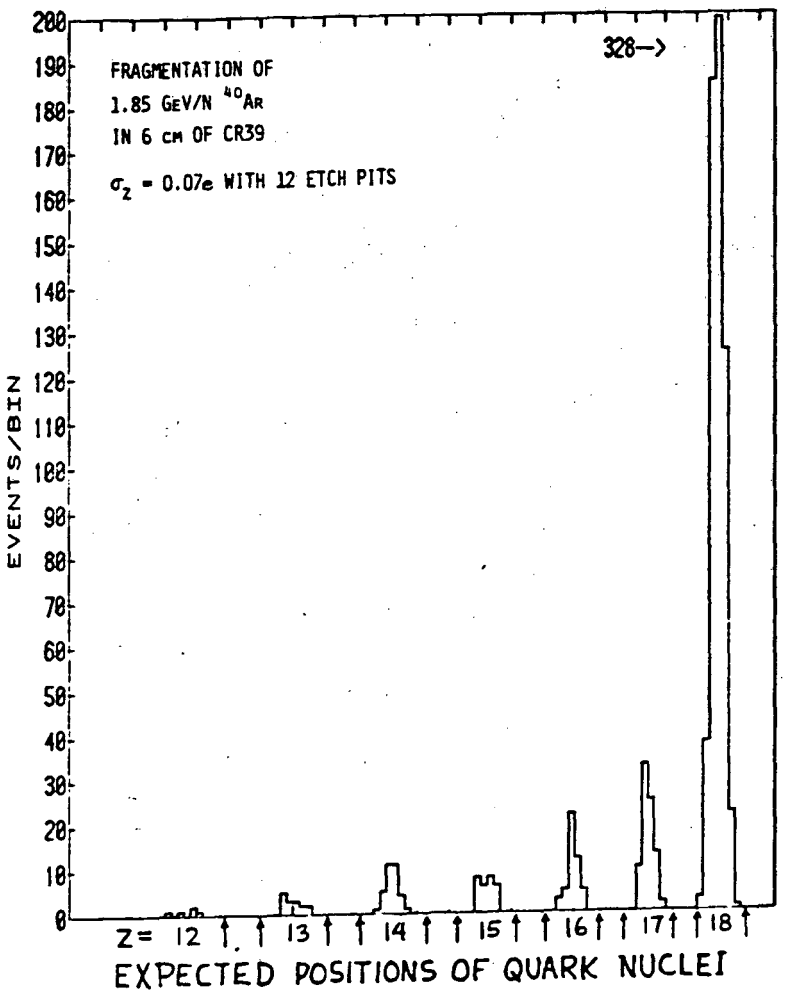
FRAGMENTATION OF
1.85 GeV/N ^{40}Ar
IN 6 cm OF CR39
σ_z = 0.07e WITH 12 ETCH PITS
328—>
EVENTS/BIN
Z= 12 13 14 15 16 17 18
EXPECTED POSITIONS OF QUARK NUCLEI

Figs. 24, 25

This report was done with support from the Department of Energy. Any conclusions or opinions expressed in this report represent solely those of the author(s) and not necessarily those of The Regents of the University of California, the Lawrence Berkeley Laboratory or the Department of Energy.

Reference to a company or product name does not imply approval or recommendation of the product by the University of California or the U.S. Department of Energy to the exclusion of others that may be suitable.

TECHNICAL INFORMATION DEPARTMENT
LAWRENCE BERKELEY LABORATORY
UNIVERSITY OF CALIFORNIA
BERKELEY, CALIFORNIA 94720